

See discussions, stats, and author profiles for this publication at: <https://www.researchgate.net/publication/24170378>

Three-Coordinate Copper(I) Amido and Aminyl Radical Complexes

ARTICLE *in* JOURNAL OF THE AMERICAN CHEMICAL SOCIETY · APRIL 2009

Impact Factor: 12.11 · DOI: 10.1021/ja809834k · Source: PubMed

CITATIONS

47

READS

50

4 AUTHORS, INCLUDING:



Neal Mankad

University of Illinois at Chicago

39 PUBLICATIONS 1,243 CITATIONS

SEE PROFILE



Robert K Szilagy

University of Pannonia, Veszprém

90 PUBLICATIONS 2,661 CITATIONS

SEE PROFILE

Published in final edited form as:

J Am Chem Soc. 2009 March 25; 131(11): 3878–3880. doi:10.1021/ja809834k.

Three-coordinate copper(I) amido and aminyl radical complexes

Neal P. Mankad¹, William E. Antholine², Robert K. Szilagyi^{3,*}, and Jonas C. Peters^{1,*}

¹ Department of Chemistry, Massachusetts Institute of Technology, Cambridge, MA 02139

² Department of Biophysics, Medical College of Wisconsin, Milwaukee WI 53226

³ Department of Chemistry and Biochemistry, Montana State University, Bozeman, MT 59717

Abstract

A three-coordinate Cu-NR₂ system (R = *p*-tolyl) supported by the anionic bis(phosphino)borate ligand [Ph₂B(CH₂P^tBu₂)₂][−] has been isolated and structurally characterized in both its anionic Cu^I and neutral (formally) Cu^{II} oxidation states. A rapid rate constant $k_S \geq 10^7 \text{ M}^{-1} \text{ s}^{-1}$ for the self-exchange electron transfer reaction makes this system a functional model for the type-1 active sites in blue copper proteins. Multi-edge XAS, multi-frequency EPR, and DFT analyses collectively indicate that the oxidized form is best regarded as a Cu^I-aminyl radical complex rather than a Cu^{II}-amido species, with about 70% localization of the unpaired electron on the NR₂ unit. Hydrogen atom transfer and C-C coupling reactions are presented as examples of chemical reactivity manifested by this unusual electronic structure.

Electron transfer (ET) through proteins often utilizes copper-containing active sites as efficient one-electron relays. The type-1 active sites of the blue copper proteins are prominent examples.^{1,2,3} It is generally thought that rapid ET rates through type-1 redox sites derive from the protein environments enforcing unusual trigonally distorted coordination spheres to allow for minimal structural reorganization during ET.^{1,4} Though large Cu^{II}/Cu^I self-exchange ET rate constants (k_S) in the range observed for type-1 sites have been achieved in certain synthetic monocopper systems using geometries distinct from trigonal environments,⁵ ET studies have yet to be conducted in a synthetic system featuring isolated, trigonally disposed copper centers. The simplest such systems would contain a trigonal planar geometry.

Here we report structural characterization of a trigonal planar system featuring formally Cu^{II} and Cu^I amido complexes related by a reversible one-electron redox event. We find in this system that ET is extremely rapid and is accompanied by a small degree of structural reorganization during redox. We propose that this structural rigidity in the absence of secondary coordination sphere effects results from significant covalency of the copper-amide linkages. In fact, a Cu^I-aminyl radical description of the formally Cu^{II} amide complex may be most appropriate.

The anionic Cu^I amido complex {[Ph₂BP^tBu₂]₂Cu(NTol)₂} {Li(12-crown-4)₂} (**1**) ([Ph₂BP^tBu₂] = Ph₂B(CH₂P^tBu₂)₂, Tol = *p*-tolyl) was synthesized by the reaction between [Ph₂BP^tBu₂]₂Cu(pyridine) and LiNTol₂ in the presence of excess 12-crown-4,⁶ and isolated as a yellow, diamagnetic solid. The cyclic voltammogram of **1** features a fully reversible redox event at −0.882 V vs FeCp₂⁺/FeCp₂ (Figure S1). Chemical oxidation of **1** with

szilagyi@montana.edu and jcpeters@mit.edu.

Supporting Information Available: Synthetic, spectroscopic, computational and EPR simulation details; ET and HAT kinetics measurements; Cu K-, Cu L-, and P K-edge data and fits. This material is available free of charge via the Internet at <http://pubs.acs.org>.

[FeCp₂][B(3,5-(CF₃)₂C₆H₃)₄] produced paramagnetic [Ph₂BP^{tBu}₂]Cu(NTol)₂ (**2**) as red needles with optical bands at 365 nm ($\epsilon = 870 \text{ M}^{-1} \text{ cm}^{-1}$) and 480 nm ($\epsilon = 600 \text{ M}^{-1} \text{ cm}^{-1}$).

Both **1** and **2** were studied by single-crystal X-ray crystallography (Figure 1; also see Figures S2–S3). Immediately evident upon comparison of the two oxidation states is the minimal degree of structural rearrangement at the Cu centers upon ET (see Figure 1B for overlay). In both structures, the Cu centers have rigorously planar coordination geometries ($\Sigma\angle = 359.97(14)^\circ$ (**1**) and $359.97(17)^\circ$ (**2**)). The Cu–P distances, P–Cu–P angles, and P–Cu–N angles are all essentially identical in both **1** and **2**. The most notable structural difference is the Cu–N contraction seen upon oxidation from **1** (2.0019(18) Å) to **2** (1.906(2) Å). The UV-Vis spectra of **2** in benzene and acetonitrile are identical (Figure S5), consistent with **2** being three-coordinate in solution as well as in the solid-state. A series of trigonal planar β -diketiminato Cu^{II} complexes synthesized by Tolman and coworkers remain the only other reported examples of three-coordinate, formally Cu^{II} complexes.⁷

Taken together, complexes **1** and **2** represent the only three-coordinate copper system to be isolated and structurally characterized in two distinct redox states.⁸ Therefore, it was of interest to study the **2/1** self-exchange ET rate constant (k_S). As discussed in the SI, we determined that k_S in this system is too large to measure accurately by NMR linewidth analysis, implying a lower limit of $k_S \geq 10^7 \text{ M}^{-1} \text{ s}^{-1}$.⁹ For comparison, blue copper proteins typically exhibit values of k_S on the order of $10^6 \text{ M}^{-1} \text{ s}^{-1}$.¹

Spectroscopic studies of the dinuclear Cu_A ET sites in cytochrome *c* oxidase and nitrous oxide reductase have revealed significant covalency in the Cu₂(μ -SR)₂ cores, resulting in significant sulfur-centered redox during ET.¹⁰ This covalency likely contributes to the extremely efficient ET rates mediated by Cu_A,¹¹ and this concept has been discussed in the context of synthetic Cu₂(μ -X)₂ model complexes.^{9,12} It is also likely that such Cu–ligand covalency likewise plays a role in the functional properties of the type-1 active sites in blue copper proteins.¹¹ We therefore sought to probe the intimate electronic structures of **1** and **2**, in particular questioning whether oxidation of the amido ligand occurs during the interchange of **1** and **2**. In other words, we wondered if the Cu^I-aminyl radical form of **2** is an important resonance contributor. A Rh complex from Grützmacher and coworkers in 2005 was the first reported example of an isolable 1:1 aminyl radical complex of a transition metal,¹³ and, unlike their aryloxy radical analogues, such complexes remain quite rare.¹⁴ To our knowledge, examples of non-chelated aminyl radical ligands have yet been reported.

Cu K-edge X-ray absorption spectroscopy (XAS) was used to probe the effective Cu oxidation states in **1** and **2**. The Cu K-edge spectra for **1** and **2** in Figure 2A show a high degree of similarity in their respective pre-edge features and rising-edge energy positions, indicating practically identical Cu effective nuclear charges and ligand fields. The first electric dipole allowed Cu 1s→4s transitions at 8982.2 eV and 8982.5 eV in **1** and **2**, respectively, are well resolved from the rising-edge features, which is indicative of trigonal planar coordination geometry.¹⁵ The small shift of 0.3 eV upon oxidation of **1** indicates that **1** and **2** have similar effective oxidation states that are closer to cuprous than cupric when compared to the reference spectra for CuCl and CuCl₂ (Figure 2A).

Cu L-edge XAS was used to directly probe the Cu 3d character of the frontier orbitals in **1** and **2**. Figure 2B compares a set of features observed at the L₃-edge for complexes **1**, **2**, CuCl, and CuCl₂. The intense pre-edge feature at 930.4 eV for CuCl₂ is due to the transition of a Cu 2p electron to the unoccupied, Cu 3d-based LUMO. The Cu 3d character of the LUMO is determined to be about 65% based upon the area under this pre-edge feature.¹⁶ This intense feature disappears in the spectrum of CuCl.¹⁷ The group of features between 936 and 937 eV in the spectrum of **1** arise due to Cu→L back-donation. Similar but more

intense features have been observed for dinuclear Cu-amidophosphine complexes.¹² Upon oxidation to **2**, a new feature at 931.9 eV appears, consistent with an electron being removed from an orbital with Cu 3d character. The proportion between the area of this feature and of the pre-edge feature in CuCl₂ indicates that the redox active molecular orbital in **2** has about 14% 3d character, and that therefore the remainder of the electron density has to be ligand-centered.

To dissect the role of the phosphine ligands in redox, we collected P K-edge XAS data (Figure 2C). In comparison to the reference PPh₃, the spectra of **1** and **2** are shifted towards higher energy due to increase in P effective nuclear charge of the phosphines involved in P→Cu donation. Upon oxidation, an electron hole is created in an orbital that has phosphorous character of about 20%.¹⁶ This with the 14% Cu 3d character clearly indicates that close to 70% of the redox active frontier orbital of **1** and **2** must have N, C, and H character. This estimate is in good agreement with spin densities calculated using DFT,¹⁸ which indicate 13% unpaired spin character on Cu, 49% on N, 15% on P, and 20% on C/H of the *p*-tolyl groups (see Figure 3 for spin density plots).

EPR spectra of **2** were collected at the S-, X-, and Q-bands (Figure 4A) and are quite unusual compared to typical cupric complexes. The S- and X-band spectra are dominated by six lines, each with several shoulders, unlike the typical four-line pattern expected for a single cupric center. Approximate simulations were obtained using the following parameters: $g_x, g_y, g_z = 2.008, 2.008, 2.030$; $A^{\text{Cu}}_x, A^{\text{Cu}}_y, A^{\text{Cu}}_z = 34, 34, 170$ MHz; $A^{\text{P}}_x, A^{\text{P}}_y, A^{\text{P}}_z = 148, 148, 173$ MHz; $A^{\text{N}}_x, A^{\text{N}}_y, A^{\text{N}}_z = 24, 100, 24$ MHz.¹⁶ Though simulation parameters are consistent with but not proof of experimental EPR parameters, reasonable fits were obtained using the same parameters at all three bands (Figure S10–S12), lending weight to their assignments. For comparison, one of Tolman's (β-diketiminato)Cu^{II}Cl complexes, a more typical three-coordinate Cu^{II} complex, has the parameters $g_{\parallel} = 2.20, g_{\perp} = 2.05, A^{\text{Cu}}_{\parallel} = 398$ MHz, $A^{\text{Cu}}_{\perp} = 52$ MHz.⁷ An example of a typical nitrogen radical is di-*t*-butylnitroxide (DTBN), which exhibits anisotropic hyperfine tensors of $A^{\text{N}} = 89.6, 16.7, \text{ and } 21.3$ MHz.¹⁹ The comparatively small A^{Cu} and large A^{N}_y values in **2**, as well as the proximity of g_{average} in **2** to the value for the free electron, indicate a significant degree of spin delocalization between the Cu and N centers.

XAS, DFT, and EPR analyses collectively suggest that **2** is better considered as a Cu^I-aminyl radical than a Cu^{II}-amido complex. This unusual electronic structure is also manifested in the chemical reactivity of the system. For instance, the addition of H-atom donors such as Bu₃SnH, PhSH, or 9,10-dihydroanthracene to solutions of **2** cleanly produced [Ph₂BP^{*t*Bu}₂]Cu(NHTol₂) (**3**). The byproducts Bu₃Sn-SnBu₃, PhS-SPh, and anthracene were detected by ¹H NMR and GC-MS, and the presence of an N-H linkage in **3** was confirmed by ¹H NMR ($\delta(\text{N-H}) = 4.93$) and IR spectroscopy ($\nu(\text{N-H}) = 3405$ cm⁻¹). The hydrogen atom transfer (HAT) reactivity of **2** is to our knowledge unprecedented for the formal Cu^{II} oxidation state. Instead, HAT reactions have been observed at Cu^{III} centers,²⁰ or alternatively, Cu^{II}-aryloxy radicals.²¹ The reaction between **2** and either Bu₃SnD or Bu₃SnH provided a kinetic deuterium isotope effect of $k_{\text{H}}/k_{\text{D}} = 4.8(6)$ at room temperature. This value is more consistent with a concerted hydrogen atom abstraction mechanism rather than rate-limiting ET followed by proton transfer, and it is within the range observed for other Cu-containing systems.²¹

Further indication of radical character delocalized into the aromatic rings in **2** comes from the oxidation chemistry of {[Ph₂BP^{*t*Bu}₂]Cu(NPh)₂}{Li(12-crown-4)₂} (**4**), which lacks methyl groups *para* to the amido nitrogen. The reaction between **4** and [FeCp₂][PF₆] produces a bright red, diamagnetic dicopper product (**5**) in which two diphenyl amido groups have been fused together at the positions *para* to the N atoms (Figure 4B; also see

Figure S4). The identity of **5** was established using a relatively low-quality X-ray crystal structure. Nonetheless, the short length of the new C-C bond (1.399(23) Å) in **5** and the planar geometries at these carbons indicate that two hydrogen atom equivalents have been lost subsequent to C-C coupling. Similar ligand-centered radical coupling has been observed in an oxidized $\text{Cu}_2(\mu\text{-NR}_2)_2$ complex¹² and from a putative three-coordinate Cu^{II} -aryloxo intermediate synthesized by Tolman.⁷

In conclusion, we have isolated and thoroughly characterized a highly covalent, three-coordinate Cu-NAr_2 system in two distinct oxidation states, with the unusual oxidized form being best regarded as an aminyl radical ligated to Cu^{I} . Chemical reactivity facilitated by this electronic structure includes HAT, C-C coupling, and efficient electron transfer, the latter being reminiscent of protein active sites bearing similar Cu coordination geometries.

Supplementary Material

Refer to Web version on PubMed Central for supplementary material.

Acknowledgments

This work was generously supported by the NSF (CHE-0750234; JCP), the ONR (N00014-06-1016; RKS), and the National Biomedical ESR Center Grant EB001980 from the NIH (WEA). NPM is grateful for an NSF graduate research fellowship. Portions of this research were carried out at the Stanford Synchrotron Radiation Lightsource, a national user facility operated by Stanford University on behalf of the U.S. DOE. The SSRL Structural Molecular Biology Program is supported by the DOE, Office of Biological and Environmental Research, and by the NIH, National Center for Research Resources, Biomedical Technology Program.

References

1. (a) Vallee BL, Williams RJP. *Proc Nat Acad Sci USA*. 1968; 59:498. [PubMed: 5238980] (b) Gray HB, Malmström BG. *Comments Inorg Chem*. 1983; 2:203.
2. (a) Ducros V, Brzozowski AM, Wilson KS, Brown SH, Ostergaard P, Schneider P, Yaver DS, Pederson AH, Davies GJ. *Nature Struct Biol*. 1998; 5:310. [PubMed: 9546223] (b) Zaitseva I, Zaitsev V, Card G, Moshkov K, Bax B, Ralph A, Lindley P. *J Biol Inorg Chem*. 1996; 1:15.(c) Karlsson BG, Nordling M, Pascher T, Tsai LC, Sjölin L, Lundberg LG. *Protein Eng*. 1991; 4:343. [PubMed: 1649999]
3. Rorabacher DB. *Chem Rev*. 2004; 104:651. [PubMed: 14871138]
4. (a) Marcus RA, Sutin N. *Biochim Biophys Acta*. 1985; 2:203.(b) Gray HB, Malmström BG, Williams RJP. *J Biol Inorg Chem*. 2000; 5:551. [PubMed: 11085645]
5. Selected examples: (a) Chaka G, Sonneberg JL, Schlegel HB, Heeg MJ, Jaeger G, Nelson TJ, Ochrymowycz LA, Rorabacher DB. *J Am Chem Soc*. 2007; 129:5217. [PubMed: 17391036] (b) Fujisawa K, Fujita K, Takahashi T, Kitajima N, Moro-oka Y, Matsunaga Y, Miyashita Y, Okamoto K. *Inorg Chem Commun*. 2004; 7:1188.
6. Mankad NP, Peters JC. *Chem Commun*. 2008:1061.
7. (a) Jazdzewski BA, Holland PL, Pink M, Young VG Jr, Spencer DJE, Tolman WB. *Inorg Chem*. 2001; 40:6097. [PubMed: 11703106] (b) Holland PL, Tolman WB. *J Am Chem Soc*. 1999; 121:7270.
8. A subset of the β -diketiminato copper(II) system studied by Tolman does access reversible 1-electron chemistry by cyclic voltammetry, but syntheses of the corresponding copper(I) complexes have not been reported. See ref 7.
9. Harkins SB, Peters JC. *J Am Chem Soc*. 2004; 126:2885. [PubMed: 14995206]
10. (a) Gamelin DR, Randall DW, Hay MT, Houser RP, Mulder TC, Canters GW, de Vries S, Tolman WB, Lu Y, Solomon EI. *J Am Chem Soc*. 1998; 120:5246.(b) DeBeer-George S, Metz M, Szilagy RK, Wang J, Cramer SP, Lu Y, Tolman WB, Hedman B, Hodgson KO, Solomon EI. *J Am Chem Soc*. 2001; 123:5757. [PubMed: 11403610]

11. (a) Solomon EI, Randall DW, Glaser T. *Coord Chem Rev.* 2000; 200–202:595.(b) Szilagyi RK, Solomon EI. *Curr Opin Chem Biol.* 2002; 6:250. [PubMed: 12039012]
12. Harkins SB, Mankad NP, Miller AJM, Szilagyi RK, Peters JC. *J Am Chem Soc.* 2008; 130:3478. [PubMed: 18298114]
13. Büttner T, Geier J, Frison G, Harmer J, Calle C, Schweiger A, Schönberg H, Grützmacher H. *Science.* 2005; 307:235. [PubMed: 15653498]
14. For a brief review, see Hicks RG. *Angew Chem, Int Ed.* 2008; 47:2. Also see: Miyazato Y, Wada T, Muckerman JT, Fujita E, Tanaka K. *Angew Chem Int Ed.* 2007; 46:5728.
15. Kau LS, Spira-Solomon DJ, Pennerhahn JE, Hodgson KO, Solomon EI. *J Am Chem Soc.* 1987; 109:6433.
16. See Supporting Information for details.
17. The small features (* in Figure 2) at 930.3 and 930.7 eV for CuCl and complex 1, respectively, are due to contamination from oxidation during shipping and handling.
18. The B(38HF)P86 functional and GT 6-311+G(d) basis set were employed. Spin densities were estimated using Mulliken population analysis.
19. Libertint LJ, Griffith OH. *J Chem Phys.* 1970; 53:1359.
20. Lockwood MA, Blubaugh TJ, Collier AM, Lovell S, Mayer JM. *Angew Chem, Int Ed.* 1999; 38:225.
21. Selected examples: (a) Thomas F, Gellon G, Gautier-Luneau I, Saint-Aman E, Pierre JL. *Angew Chem, Int Ed.* 2002; 41:3047.(b) Chaudhuri P, Hess M, Weyhermüller T, Wieghardt K. *Angew Chem, Int Ed.* 1999; 38:1095.(c) Wang Y, DuBois JL, Hedman B, Hodgson KO, Stack TDP. *Science.* 1998; 279:537. [PubMed: 9438841]

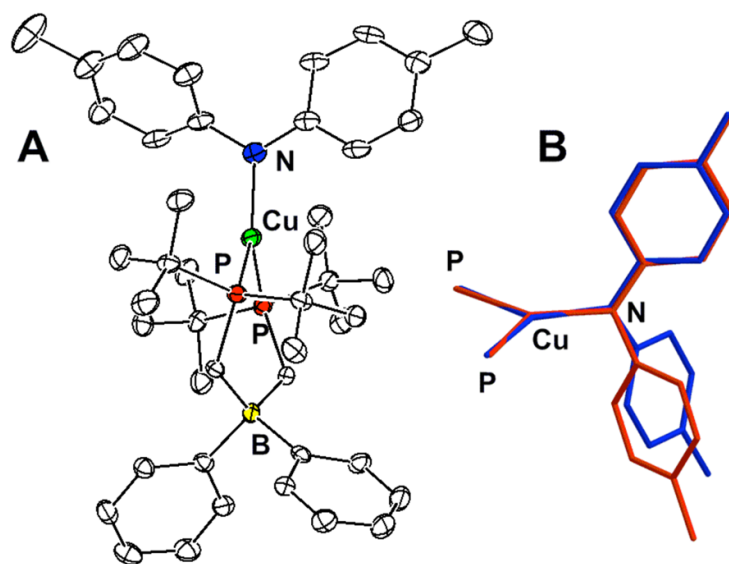
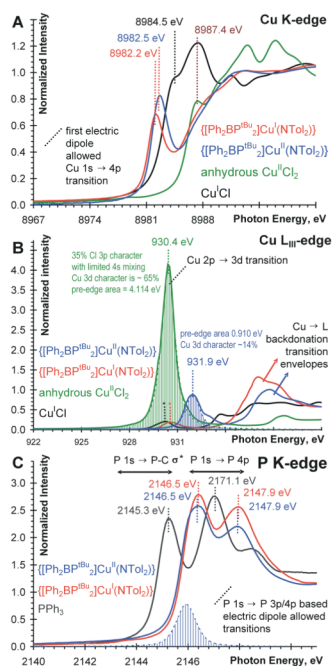


Figure 1.

A) Solid-state structure of **2**. B) Structural overlay of anion **1** (red) and **2** (blue) with only phosphorus atoms of [Ph₂BP^tBu₂] shown.

**Figure 2.**

A) Cu K-edge spectra and B) Cu L₃-edge spectra and C) P K-edge spectra of CuCl (black), **1** (red), CuCl₂ (green), **2** (blue), and PPh₃ (gray). * = trace impurity

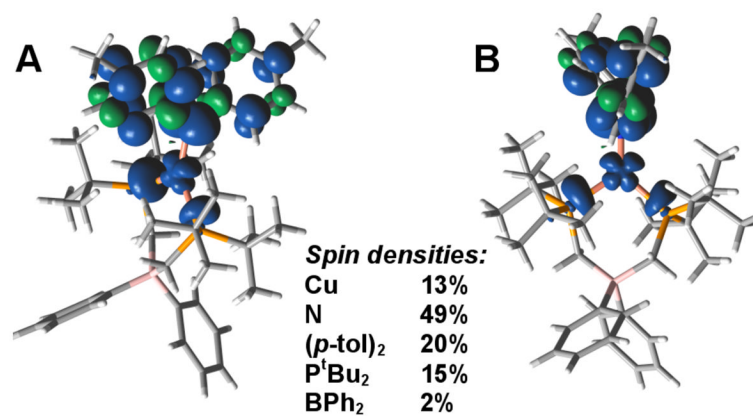


Figure 3. Atomic spin density plots¹⁸ (0.002 isocontours) for [Ph₂BP^{*t*}Bu₂]₂Cu(NTol)₂ viewed A) parallel and B) perpendicular to the P₂CuN plane.

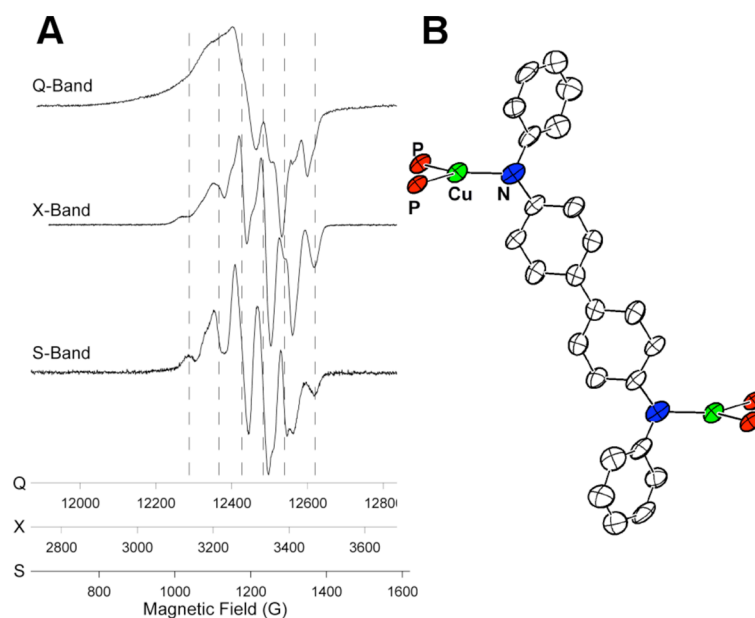


Figure 4.

A) Multifrequency EPR spectroscopy of **2**. Spectra were recorded in a frozen dichloromethane/toluene glass. Microwave frequency (temperature): 35.100 GHz (123 K), 9.188 GHz (77 K), and 3.392 (123 K) for Q-, X-, and S-band, respectively. B) Core structure of **5**, with only phosphorus atoms of $[\text{Ph}_2\text{BP}^{\text{tBu}}_2]$ shown.